IONIZED PHOTOEVAPORATION FLOWS IN H II REGIONS AND PNe[1]

W. J. Henney

Instituto de Astronomía, UNAM

RESUMEN

Desde los *proplyds* hasta los flujos de champán, a través de 4 órdenes de magnitud en tamaño y densidad, los flujos fotoevaporativos son ubicuos en regiones H II. También se encuentran dichos flujos en las nebulosas planetarias, en la forma de nudos cometarios, aunque en este caso los flujos suelen ser "dominados por advección", a diferencia de los flujos "dominados por recombinación" que predominan en regiones H II. Se discuten las propiedades generales de tales flujos, con referencia particular a resultados recientes sobre los *proplyds* de Orión y los nudos de la Hélice.

ABSTRACT

From proplyds to champagne flows, spanning 4 orders of magnitude in size and density, photoevaporation flows are ubiquitous in H II regions. Such flows are also found in planetary nebulae, in the form of cometary knots, although in this case the flows are often "advection–dominated", unlike the "recombination–dominated" flows that predominate in H II regions. The general properties of such flows are discussed, with particular reference to recent results on the Orion proplyds and the Helix knots.

Key Words: **H II REGIONS — PLANETARY NEBULAE**

The name proplyd is given to circumstellar disks and envelopes around young low–mass stars that are revealed by the presence of intense ultraviolet radiation from nearby massive stars (e.g. O'Dell 1998; Bally et al. 1998; Henney & O'Dell 1999, hereafter HO99). They fall into two classes: the bright proplyds, visible as compact emission line knots due to the photoevaporation and subsequent ionization of the circumstellar disk (Johnstone, Hollenback & Bally 1998; Henney & Arthur 1998, hereafter HA98), and the dark proplyds, whose dusty disks are seen in extinction against the emission of the ionized gas that lies behind them (McCaughrean & O'Dell 1996). The proplyds were first detected in the Orion nebula (Laques & Vidal 1979; O'Dell, Wen & Hu 1993), but have since been found in other H II regions (Stapelfeldt et al. 1997; Stecklum et al. 1998; Brandner et al. 2000), although those in Orion remain by far the most numerous (O'Dell & Wong 1996).

However, even within the Orion nebula, the proplyds are not the only photoevaporation flows. The nebula itself is probably one large champagne flow, accelerating away from the background molecular cloud, while smaller scale flows stream off the Orion bar and other similar features (see O'Dell, this volume). Turning to other H II regions, photoevaporation flows are ubiquitous, from "elephant trunks" to "cometary globules" (Pottasch 1956; Schmidt 1974; Bertoldi 1989; Bertoldi & McKee 1990). Indeed, it has been argued (Hester et al. 1996; Scowen et al. 1998) that *all* optically visible H II regions in our own and other galaxies are largely photoevaporation flows. Finally, similar phenomena are seen in planetary nebulae (PNe). Such "cometary knots" have been most extensively studied in the Helix nebula (Meaburn et al. 1992; O'Dell & Handron 1996), but are also found in other PNe (O'Dell, Weiner, & Chu 1990; Meaburn & Lopez 1993).

In this paper, I first review the current status of photoevaporation models for the Orion proplyds. I then discuss some general properties of photoevaporation flows and the different regimes in which they may operate. This leads to an important distinction being drawn between the "recombination–dominated" flows common in H II regions and the "advection–dominated" flows found in nearby PNe, some observational consequences of which are outlined in the last section.

---

[1]Based in part on observations with the NASA/ESA Hubble Space Telescope, obtained at the Space Telescope Science Institute, which is operated by the Association of Universities for Research in Astronomy, Inc., under NASA Contract No. NAS 5–26555.

1. PHOTOEVAPORATION MODELS OF PROPLYDS

The models described here (see HO99) employ semi–analytic calculations of the dynamics and photoion-ization equilibrium of the transsonic photoevaporation flow (Dyson 1968; Bertoldi 1989) from a D–critical ionization front (IF), whose shape is specified a priori. Both the direct ionizing radiation from a high–mass star and the diffuse ionizing radiation from the surrounding H II region are accounted for, and the IF is assumed hemispherical on the side facing towards the ionizing star (proplyd head) and cylindrical on the side facing away from it (proplyd tail). The results are broadly consistent with more sophisticated numerical radiation–hydrodyamic simulations (Richling & Yorke 1998; 2000), which self–consistently model both the neutral and ionized parts of the photoevaporation flow, starting from the surface of the circumstellar disk.

The most important model parameters are the peak density, n_0, in the ionized flow and the radius, r_0, of the forward–facing ionization front. Secondary parameters are the inclination, i, between the proplyd axis and the observer's line of sight, the relative strength, β, of the diffuse field, and the length, ℓ of the proplyd tail. If the proplyd is spatially well–resolved then the peak observed linear emission measure (EM) is $\simeq 0.2n_0^2 r_0 \cos i$, although for unresolved proplyds this quantity will be smaller. In the absence of dust extinction, the Balmer line intensity of the proplyd will be proportional to EM, whereas the Balmer line flux will be proportional to the volume emission measure (VEM), which is $\simeq 1$–$2n_0^2 r_0^3$, depending on the relative brightness of the tail, but independent of angular resolution. These were the bases for the determination of n_0 and r_0 by fitting models to HST WFPC2 Hα images (HA98). It turns out that the inclination, i, is not very well constrained by such fitting, although i can be determined with much better precision by using the model–predicted kinematics to fit emission line spectral profiles (HO99).

In the course of work on the radio emission of proplyds (Henney, García-Díaz, & Kurtz, these proceedings), we have discovered an error in the Hα emissivity used by HA98, which results in their values of n_0 being overestimated by $\simeq 50\%$. This error is also present in HO99, meaning that the mass–loss rates given in that paper are $\simeq 50\%$ too large. However, the qualitative results of neither paper are changed.

Using the correct emissivity value gives typical peak densities of $n_0 = 10^6$–10^7 cm^{-3} for the proplyds that lie within a projected angular distance of $10''$ (6.5×10^{16} cm at a distance of 430 pc) of the principal ionizing star of the nebula, θ^1 C Ori. These proplyds have typical IF radii of $r_0 = 10^{14}$–10^{15} cm (7–65 AU), whereas more distant proplyds tend to be somewhat larger ($r_0 = 1$–2×10^{15} cm) and lower density ($n_0 = 10^5$–10^6 cm^{-3}).

2. CLASSIFICATION OF PHOTOEVAPORATION FLOWS

The dynamic ionization balance in a photoevaporation flow can be approximately expressed by the formula $F_* \simeq u n_0 + \alpha n_0^2 h$, where F_* is the ionizing photon flux incident on the outside of the flow, n_0 is the peak ionized density in the flow, u is the initial velocity of the flow, α is the recombination coefficient, and h ($\simeq 0.1 r_0$) is the effective thickness of the flow (e.g. Bertoldi 1989). From this equation, one can identify two regimes, depending on which of the two terms on the RHS predominates. If it is the first term, then one finds an "advection–dominated" flow, in which the majority of incident ionizing photons reach the IF and ionize fresh gas, whereas if the second term dominates, then one has a "recombination–dominated" flow, in which the majority of ionizing photons are used up in balancing recombinations in the flow, resulting in very few reaching the IF.

The dividing line between these two regimes is $n_0 \simeq 4 \times 10^{18} h^{-1}$ for the common case in which $u \simeq c_0 \simeq 10$ km s^{-1} and $\alpha = \alpha_{\rm B} \simeq 2.6 \times 10^{-13}$ cm^3 s^{-1}. This is shown in Figure 1, together with the regions of the n_0-h plane occupied by observed flows in H II regions and PNe. It can be seen that the majority of proplyds and other H II region flows, such as champagne flows, elephant trunks, and cometary globules, fall along a well–defined "main sequence", which lies roughly parallel to the advection/recombination dividing line, but substantially above it, inside the recombination–dominated region. The cometary knots in PNe, however, lie well below the line, inside the advection–dominated region (apart from the knots in the Eskimo, NGC 2392). Also shown in the figure are contours of constant ionizing photon flux, F_* (erg s^{-1} cm^{-2}), which follow $n_0 \propto h^{-1/2}$ in the recombination–dominated zone and are flat ($n_0 = $ constant) in the advection–dominated zone. Interestingly, the H II region main sequence is steeper than the lines of constant F_* due to the tendency for the more compact photoevaporation flows to lie closer to the ionizing star, where the flux is higher.

It is chiefly the low ionizing luminosity of PN central stars, as compared to O stars, that leads to advection–
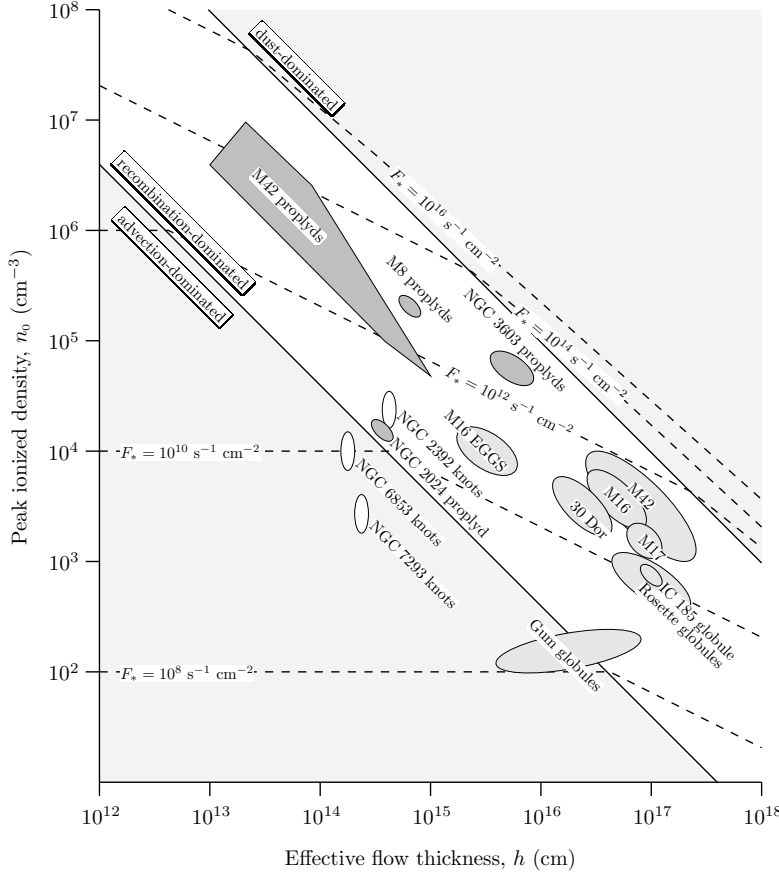
Fig. 1. Peak density versus thickness for photoevaporation flows in H II regions and PNe. Shapes with the darkest shading indicate proplyds, while lighter shading shows cometary globules, elephant trunks and champagne flows. Unshaded shapes indicate PNe cometary knots. Dashed lines show contours of constant ionizing flux, F_*, and solid lines mark the boundaries between different photoevaporation regimes. Flow parameters were taken from the literature (see text for references), except for the M42 proplyds and the NGC 6853 and NGC 2392 knots, which were estimated from publicly-available HST Hα images using the flux calibration of O'Dell & Doi (1999).

dominated flows from the knots in the Helix (NGC 7293) and Dumbbell (NGC 6833) nebulae. The borderline cases in H II region flows can also be ascribed to a low ionizing flux, due to being ionized by a B0 star in the case of the NGC 2024 proplyd (Stapelfeldt et al. 1997) and to the large separation ($\simeq 50$ pc) from the ionizing source in the case of the Gum globules.

Including the effects of dust opacity in the ionization balance equation (e.g. Pastor, Cantó, & Rodríguez 1991) allows the delineation of a further zone in the n_0-h plane, in which most ionizing photons are absorbed by dust. For standard galactic dust properties (Bertoldi & Draine 1996), dust–dominated flows will arise for $n_0 > 10^{21} h^{-1}$, but it can be seen from the figure that there are no observed flows in this region.

3. OBSERVATIONAL DIFFERENCES BETWEEN THE TWO FLOW REGIMES

In recombination–dominated flows, the surface brightness in a recombination line such as Hα is directly proportional to the incident ionizing flux, a fact that was taken advantage of by Wen & O'Dell (1995) to construct a 3–dimensional model of the principal IF in Orion. However, in advection–dominated flows, this is no longer true and the Hα surface brightness falls below the value one would predict from the ionizing flux. In the case of the Helix knots, this discrepancy was first noted by O'Dell & Handron (1996), and photoevaporation flow models were finally reconciled with the observed surface brightness by López-Martín et al. (2000).

A further difference between recombination– and advection–dominated flows is that in the former case, the IF transition is much thinner than the effective thickness, h, of the flow, whereas in the latter case the two thicknesses are roughly equal. That the distinction between a thick/thin IF should approximately coincide with the distinction between advection/recombination flows is due to the accidental fact that the sound speed in photoionized gas is usually of the same order as the recombination rate divided by the effective absorption cross–section. As a result, recombination–dominated flows are expected to have H fully ionized throughout and to be approximately isothermal (save for the effects of hardening and collisional deexcitation). Advection–dominated

flows, on the other hand, should show strong gradients in H ionization fraction and temperature.

Just such a behaviour is found in the Helix cometary knots (O'Dell, Henney, & Burkert 2000), where the relative distribution of the Hα and forbidden [N II] emission appears at first sight to be contrary to the predictions of photoionization models. One normally expects to only find [N II] emission close to the IF, in a thin H$^+$/He^0 zone, with Hα emission being more spatially extended. This is indeed the case in the Orion proplyds, as can be appreciated in Figure 2 (see Plate 1), but in the Helix knots the opposite is found, with the Hα emission lying inside (with respect to the knot) the [N II] emission. Such behaviour can be fully explained, however, by the temperature–dependence of the Hα and [N II] emissivities. The inner regions of the photoevaporation flow have a lower ionization fraction and are cooler, which augments the emissivity of recombination lines while simultaneously reducing the emissivity of collisionally excited lines such as [N II]. Indeed, O'Dell et al. (2000) show that a simple photoevaporation model is very successful in reproducing the spatial distribution of different emission lines.

REFERENCES

Bally, J., Sutherland, R. S., Devine, D., & Johnstone, D. 1998, AJ 116, 293

Bertoldi, F., 1989, ApJ, 346, 735

Bertoldi, F., & Draine, B. T. 1996, ApJ, 458, 222

Bertoldi, F., & McKee, C. F. 1990, ApJ, 354, 529

Brandner, W., Grebel, E. K., Chu, Y-H., Dottori, H., Brandl, B., Richling, S., Yorke, H. W., Points, S. D., & Zinnecker, H. 2000, AJ, 119, 292

Dyson, J. E. 1968, Ap&SS, 1, 388

Henney, W. J., & Arthur, S. J. 1998, AJ, 116, 322 (HA98)

Henney, W. J., & O'Dell, C. R. 1999, AJ, 118, 2350 (HO99)

Hester, J. J., et al. 1996, AJ, 111, 2349

Johnstone, D., Hollenbach, D., & Bally, J. 1998, ApJ, 499, 758

Laques, P., & Vidal, J. L. 1979, A&A, 73, 97

López-Martín, L., Raga, A. C., Mellema, G., Henney, W. J., & Cantó, J. 2000, MNRAS, in press

McCaughrean, M. J., & O'Dell, C. R, 1996, AJ, 111, 1977

Meaburn, J., & Lopez, J. A. 1993, MNRAS, 263, 890

Meaburn, J., Walsh. J. R., Clegg, R. E. S., Walton, N. A., Taylor, D., & Berry, D. S. 1992, MNRAS, 255, 177

O'Dell, C. R. 1998, ApJ, 115, 263

O'Dell, C. R. & Doi, T. 1999, PASP, 111, 1316

O'Dell, C. R. & Handron, K. D. 1996, AJ, 111, 1630

O'Dell, C. R., Henney, W. J., & Burkert, A. 2000, AJ, 119, 2910

O'Dell, C. R., Weiner, L. D., & Chu, Y.-H. 1990, ApJ, 362, 226

O'Dell, C. R., Wen, Z., & Hu, X. 1993, ApJ, 410, 696

O'Dell, C. R. & Wong, S. K. 1996, AJ, 111, 846

Pastor, J., Cantó, J., & Rodríguez, L. F. 1991, A&A, 246, 551

Pottasch, S. R. 1956, BAIN, 13, 77

Richling, S. & Yorke, H. W. 1998 A&A 340, 508

Richling, S. & Yorke, H. W. 2000 A&A in press

Schmidt, E. G. 1974, MNRAS, 169, 97

Scowen, P. A., et al. 1998, AJ, 116, 163

Stapelfeldt, K., Sahai, R., Werner, M., & Trauger, J. 1997, in ASP Conf. Ser. 119, Planets beyond the Solar System and the Next Generation of Space Missions, ed. D. R. Soderblom (San Francisco: ASP), 131

Stecklum, B., Henning, T., Feldt, M., Hayward, T. L., Hoare, M. G., Hofner, P., & Richter, S. 1998, AJ, 115, 767

Wen, Z. & O'Dell, C. R. 1995, ApJ, 438, 784

W. J. Henney: Instituto de Astronomía, Universidad Nacional Autónoma de México, Campus Morelia, Apartado Postal 3–72 (Xangari), 58089 Morelia, Michoacán, México (will@astrosmo.unam.mx).

![Color–coded HST WFPC2 images of Orion proplyds and Helix knots](image)

10^{16} cm

2×10^{15} cm

NGC 7293 428–900

2×10^{15} cm

NGC 7293 352–815

M42 244–440

2×10^{15} cm

2×10^{15} cm

2×10^{15} cm
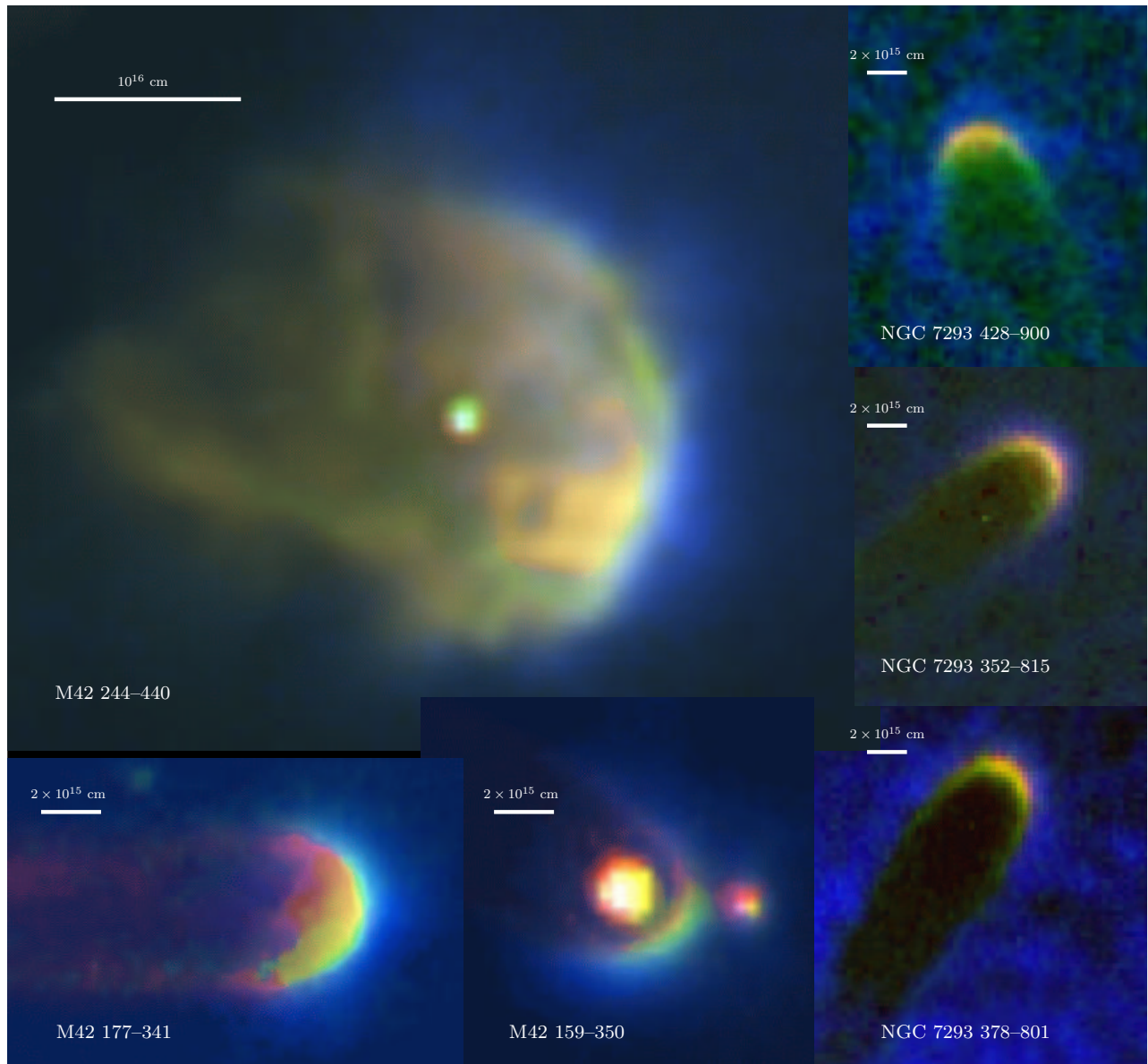
M42 177–341

M42 159–350

NGC 7293 378–801

Fig. 2. Color–coded HST WFPC2 images of 3 of the largest Orion proplyds (left) and 3 typical Helix knots (right) in 3 emission line filters: [N II] 6583Å (red), Hα (green), and [O III] 5007Å (blue). For each object, the white bar indicates the approximate value of the ionization front radius. The color saturation has been artificially enhanced to bring out the contrast between different emission zones. The proplyds show the classic ionization stratification, with an inner [N II] zone enclosed in an outer [O III] zone, with Hα straddling both zones. This results in a red–yellow–green–blue rainbow arc in the proplyd cusp. In the Helix knots, on the other hand, the Hα emission peaks inside that of [N II], giving rise to a green–yellow–red–blue sequence in the cusp.